

Research article

Construction and drug screening of Co-culture system using extrahepatic cholangiocarcinoma organoids and tumor-associated macrophages

Yinghao Guo^{a,1}, Qi Li^{a,1}, Qinghuang Ye^a, Yun Jin^a, Yuanquan Yu^a, Xiaoxiao Zhang^a, Longfu Xi^a, Yihang Wang^a, Di Wu^a, Yanzhi Pan^a, Shumei Wei^b, Qingyong Li^c, Huiquan Wang^d, Jiangtao Li^{a,*}

^a Department of Surgery, The Second Affiliated Hospital, Zhejiang University School of Medicine, Hangzhou, 310009, Zhejiang Province, China

^b Department of Pathology, The Second Affiliated Hospital, Zhejiang University School of Medicine, Hangzhou, 310009, Zhejiang Province, China

^c College of Pharmaceutical Science, Zhejiang University of Technology, Hangzhou, 310014, Zhejiang Province, China

^d Micro-Satellite Research Center, Zhejiang University, Hangzhou, 310027, Zhejiang Province, China

ARTICLE INFO

Keywords:

Extrahepatic cholangiocarcinoma
Organoids
Tumor-associated macrophages
Genetic profiles
Therapy resistance

ABSTRACT

Patient-derived organoids (PDOs) have been proposed as a novel in vitro tumor model that can be applied to tumor research and drug screening. However, current tumor organoid models lack components of the tumor microenvironment, particularly tumor-associated macrophages (TAMs). We collected peripheral blood and tumor samples from 6 patients with extrahepatic cholangiocarcinoma (eCCA). Monocytes were induced into TAMs by cytokine and conditioned medium, and then co-cultured with tumor organoids. Our comprehensive analysis and comparison of histopathology and genomics results confirmed that this co-culture model can better capture intra- and inter-tumor heterogeneity retain the specific mutations of the original tumor. Drug sensitivity data in vitro revealed that gemcitabine and cisplatin are effective drugs for cholangiocarcinoma, but TAMs in the tumor microenvironment promote organoids growth and chemotherapy resistance. In conclusion, our organoid model of cholangiocarcinoma co-cultured with TAMs can not only shorten the model construction cycle, but also preserve the heterogeneity of original tumors to improve the accuracy of drug screening, and can also be applied to the researches of TAMs and tumors.

1. Introduction

The tumor microenvironment of eCCA contains a number of cell types, including TAMs, tumor-associated neutrophils, cancer-associated fibroblasts, regulatory T lymphocytes, and endothelial cells [1,2]. In eCCA, TAMs are a group of highly infiltrative immune cells that promote tumor progression and immunosuppression [2]. In the past, macrophages were divided into two types according to their cell state: classically activated (M1) and alternately activated (M2); M1 macrophages were characterized by CD86 and iNOS, while M2 macrophages were characterized by CD206 and CD163 [3]. However, since macrophage polarization is a dynamic

* Corresponding author.

E-mail address: zrljt@zju.edu.cn (J. Li).

¹ Both authors contributed equally to this work.

process, it is difficult to define TAMs specifically in the eCCA microenvironment [4]. Nonetheless, researchers generally agree that TAMs present with the M2 phenotype; previous studies have found that TAMs secrete a variety of growth factors and produce a variety of proteolytic enzymes to promote CCA occurrence, invasion and metastasis, but they also release immunosuppressive molecules resulting in therapeutic resistance [5–7]. Due to the high heterogeneity of eCCA, the research progress on the microenvironment has been slow.

Although eCCA heterogeneity is incompletely understood, the advent of PDOs has promoted the development of precision therapy for eCCA. Organoids are a type of three-dimensional cell-culture technology derived from tumor stem cells in vitro. Compared with traditional 2D tumor cell lines, organoids retain histopathologic features, such as phenotype, genetic diversity, and mutation signals, of the original tumor tissues [8]. The patient-derived tumor xenograft (PDX) model remains the only system that preserves the microenvironment and heterogeneity of tumors, but its use is limited due to its high cost, long culture cycles, and low success rates in clinical application. In contrast, organoids can be expanded on a large scale and preserved long-term, which could contribute to the construction of tumor organoid biobanks and provide a platform for high-throughput drug screening [9,10]. Unfortunately, current organoids cannot capture the tumor microenvironment with fibroblasts and immune cells, which limits their reproducibility, as well as the accuracy of drug screening [11]. Previous studies have partially addressed this challenge by co-culturing tumor organoids with a variety of cells. Seino et al. co-cultured pancreatic ductal adenocarcinoma organoids with CAFs and found that CAF-derived Wnt yielded growth of a new pancreatic ductal adenocarcinoma subtype [12]. Additionally, Dijkstra et al. obtained tumor-specific T cells with a co-culture model of tumor organoids and peripheral blood lymphocytes, and immunotherapy sensitivity or resistance factors were also produced by the tumor organoids [13].

Our group has successfully constructed dozens of CCA organoids and verified the accuracy of the drug sensitivity of these organoid models [14,15]. Here, for the first time, we developed a 3D co-culture system using organoids from eCCA and TAMs. With this system, we compared the reduction degree of the model with that of the source tissue, and we describe the effects of TAMs on organoid growth and chemotherapy resistance.

2. Materials and methods

2.1. Specimen collection

The study adhered to the tenets of the Declaration of Helsinki and was approved by the ethics committee of the Second Affiliated Hospital, Zhejiang University, School of Medicine (No. 2019-408). In order to exclude the influence of other tumor treatments on the construction and subsequent application of the organoid model, we selected patients with untreated cholangiocarcinoma before surgery, and then collected surgical samples from patients with cholangiocarcinoma who underwent radical cholangiocarcinoma resection in the Department of Hepatobiliary and Pancreatic Surgery of the Second Affiliated Hospital of Zhejiang University to ensure that the sample collection time from tissue was less than 30 min. The samples were stored in tissue preservation solution at 4 °C before transport. Each tumor specimen was divided quickly into three parts after harvesting. One part was collected in cold PBS and transported on ice to the laboratory for tumor stem cell isolation and organoid culture. The other two parts were placed in liquid nitrogen and tissue fixation solution for sequencing and histopathological analysis. At the same time, 10–12 mL of peripheral blood from the same cholangiocarcinoma patient was taken during the operation for subsequent isolation and acquisition of monocytes. Subsequently, clinical data of patients with cholangiocarcinoma were collected from the medical record system, including magnetic resonance imaging data and postoperative follow-up information.

2.2. Tumor cell isolation and organoid culture

CCA tissues were initially washed three times with cold PBS and cut into 1-mm³ pieces using ophthalmic scissors. Then, the tissue fragments were digested in 10 mL digestion medium containing advanced Dulbecco's modified Eagle's medium/F12 (Gibco, CA, USA) and 15 mg collagenase D (Roche, Basel, Switzerland) for 3 h at 37 °C. Next, the digestion status of the tissue fragments was checked under a microscope after repeated mixing with digestion medium. Then, the cell suspensions were filtered through a 100- μ m cell strainer and centrifuged at 300 \times g for 5 min at room temperature. The tumor cells were resuspended in culture medium at a concentration of 5×10^5 cells/mL. Growth factor-reduced Matrigel matrix (Corning, NY, USA) was used to culture CCA organoids. Matrigel was mixed with the cell suspensions in a 1:1 ratio, and 200 μ L of the mixtures were seeded in pre-coated 24-well plates. Finally, organoid culture medium (Advanced DMEM/F12 supplemented with 1 % penicillin/streptomycin (1 \times , ThermoFisher, MA, USA), Glutamax (1 \times ; ThermoFisher), B27 supplement (1 \times ; Gibco, CS, USA), N2 supplement (1 \times ; Gibco, CS, USA), HEPES (10 mM, ThermoFisher, MA, USA), gastrin (10 nM; Sigma Aldrich, MO, USA), A83-01 (5 μ M; Tocris, Bristol, UK), Y-27632 (10 μ M; Tocris, Bristol, UK), recombinant human epidermal growth factor (50 ng/mL; PeproTech, NJ, USA), recombinant human fibroblast growth factor 10 (100 ng/mL; PeproTech), recombinant human R-Spondin1 (500 ng/mL; PeproTech), recombinant human Noggin (100 ng/mL; PeproTech), and Afamin/Wnt3a CM (10 % v/v; MBL Life Science, TKY, Japan) was added (500 μ l per well) and changed every 3 days.

2.3. Peripheral blood monocyte isolation and differentiation

Isolation: Peripheral blood mononuclear cells (PBMCs) were isolated from peripheral blood samples of patients with cholangiocarcinoma by density gradient centrifugation, such as using Ficoll density gradient centrifugation (Solarbio, Beijing, CHN).

Culture: Isolated PBMCs were cultured in culture flasks containing RPMI 1640 and 10 % fetal bovine serum (FBS). To promote the differentiation of monocytes into macrophages, it is usually necessary to add 20 ng/mL macrophage colony-stimulating factor (M-CSF) to the medium.

Differentiation: when PBMCs were cultured to approximately 70–80 % confluency, the medium was removed and replaced with a new medium containing M-CSF to promote differentiation of monocytes into macrophages. It usually takes 5 days to complete the differentiation process, during which the medium containing M-CSF needs to be replaced. Once macrophage differentiation is complete, polarization toward M2 can be induced by the addition of specific tumor conditioned media, and culture is generally continued for 48 h after the addition of these factors to ensure that macrophages successfully acquire the M2 phenotype.

Identification: The expression of M2 macrophage-specific protein (CD206) was observed by immunofluorescence staining.

2.4. Co-culture of CCA organoids and TAMs

To achieve co-culture of cholangiocarcinoma organoids and tumor-associated macrophages, we used a Transwell system (3470, Corning, NY, USA) with a 0.4 μm filter pore size to retain the two types of cells to interact through the secretion of multiple cytokines and chemokines. To be specific, 1×10^5 TAMs were seeded on a membrane insert in a Transwell chamber, and 5×10^5 organoids were seeded into the lower compartment of 24-well plates for 14 days.

2.5. Patient-derived organoid xenograft experiments using organoids and TAMs

All the experimental mice were purchased from Jiangsu Zhizhuo Yaokang Biotechnology Company. Four-to six-week-old NSG mice were selected to establish the patient-derived organoid xenograft (PDOX) model. Five mice in each group were selected to inject whole organoids (5×10^5) or organoids containing TAMs (1×10^5) suspended in 100 μL Matrigel subcutaneously in the flanks. Tumor sizes and weights were measured 8 weeks later, and all the mice were euthanized, the tumors were removed, immobilized in paraformaldehyde overnight, and then immunostaining was performed. All animals received humane care according to the standards set out in the "Guidelines for the Care and Use of Laboratory Animals."

2.6. Histology and staining

Matrigel was digested with dispase II (1.5 mg/mL; Roche, Basel, Switzerland) for up to 1 h at 37 °C. Organoids were harvested after centrifuging at $300 \times g$ for 5 min at room temperature. Then, the original specimens and organoids were fixed in 4 % paraformaldehyde and embedded in paraffin. Five-micrometer-thick sections were prepared for HE and immunohistochemical staining. Then, the sections were incubated with anti-cytokeratin 7 (CK7; Abcam, Cambridge, UK, 1:2000) anti-mucin-1 (MUC1; Abcam, Cambridge, UK, 1:500), and anti-epithelial cell adhesion molecule (EpCAM; Abcam, Cambridge, UK, 1:500) primary antibodies in a blocking solution in a wet chamber overnight at 4 °C. Staining was obtained using 3,3'-diaminobenzidine as the chromogen, followed by hematoxylin counterstaining.

TAMs were fixed in 4 % paraformaldehyde for 1 h at 4 °C; then, 100 μL of Triton X-100 was added (0.5 % Triton X-100) and incubated at room temperature for 20 min. Subsequently, the TAMs were blocked for 1 h at room temperature in blocking buffer. Mouse monoclonal antibodies targeting CD68 (Abcam, Cambridge, UK, 1:500), α -SMA (Abcam, Cambridge, UK, 1:200), CD31 (Abcam, Cambridge, UK, 1:200), and CD206 (Abcam, Cambridge, UK, 1:500) were utilized as primary antibodies, while goat anti-mouse IgG H&L (Alexa Fluor® 647) was utilized as the secondary antibody.

2.7. Drug screening

Organoids were incubated with 0.25 % trypsin and 0.02 % EDTA at 37 °C for 5 min; then, the dissociated cells were resuspended in Advanced DMEM with 2 % Matrigel and seeded in 384-well plates at 100–200 cells in 22.5 μL per well. Following 48 h of culture, the medium was replaced with complete culture medium supplemented with 0.01, 0.1, 1, 10, or 50 μM of gemcitabine, 5-fluorouracil, cisplatin, and paclitaxel. After incubation at 37 °C for 96 h, cell viability was measured with a CellTiter-Glo assay (Promega, WI, USA). Wells of complete culture medium without drug was used as a negative control, and assay was done in triplicate wells, and each experiment was repeated two times. For the comparison of drug sensitivity of eCCA organoids, drug dose-response curves and IC50 values were generated by nonlinear regression fitting to a three-parameter model with 100 % and 0 % cell viability as constraints.

2.8. Whole-exome sequencing (WES)

Total genomic DNA from the original tumors and organoids was extracted using a GenElute Mammalian Genomic DNA miniprep kit (Sigma, MO, USA). WES was carried out on Illumina platforms. SAMtools mpileup and bcftools were used for variant calling and to identify SNP and INDEL variants. Somatic SNV was detected by muTect, somatic INDEL was detected by Strelka, and somatic CNV was detected by control-FREEC.

2.9. Statistical analysis

All statistical analyses were performed using GraphPad Prism software 7.0 (GraphPad Software, CA, USA).

3. Results

3.1. Extrahepatic cholangiocarcinoma organoids and TAMs Co-culture system

To mimic the eCCA tumor microenvironment, we first constructed 3D co-culture systems using eCCA organoids and TAMs (Fig. 1A). We successfully established 6 eCCA tumor organoids from surgical resection as previously described. The clinical characteristics of the 6 eCCA patients are presented in Table 1. All tumor pathological types were adenocarcinoma; most tumors were moderately differentiated, but 2 cases were poorly differentiated. Further analysis showed no differences in the success rate of organoid culture attributed to clinical parameters, but there were differences associated with the initial acquisition of the tumor stem cells. TAMs were isolated and differentiated from the peripheral blood of each patient. Immunofluorescence staining confirmed that most TAMs were CD206-positive, and a small number of cells were CD86-positive. The presence of other cell types, such as CAFs and endothelial cells, was excluded according to the corresponding markers α -SMA and CD31 (Supplement 1). Finally, we selected an indirect contact Transwell system to mimic the tumor microenvironment. In this system, eCCA organoids were seeded on the bottom layer, and TAMs were seeded on the upper layer (Fig. 1B).

3.2. Co-culture system using eCCA organoids and TAMs preserved the histopathological structures of tumors

As with gastrointestinal and lung organoids, eCCA organoids cultured alone and co-cultured with TAMs preserved the histopathological features of the source tissue. The eCCA organoids varied greatly in growth rate and morphology, but they retained tissue heterogeneity, whether cultured alone or co-cultured. According to H&E staining (Fig. 2A and B), all eCCA organoids retained the

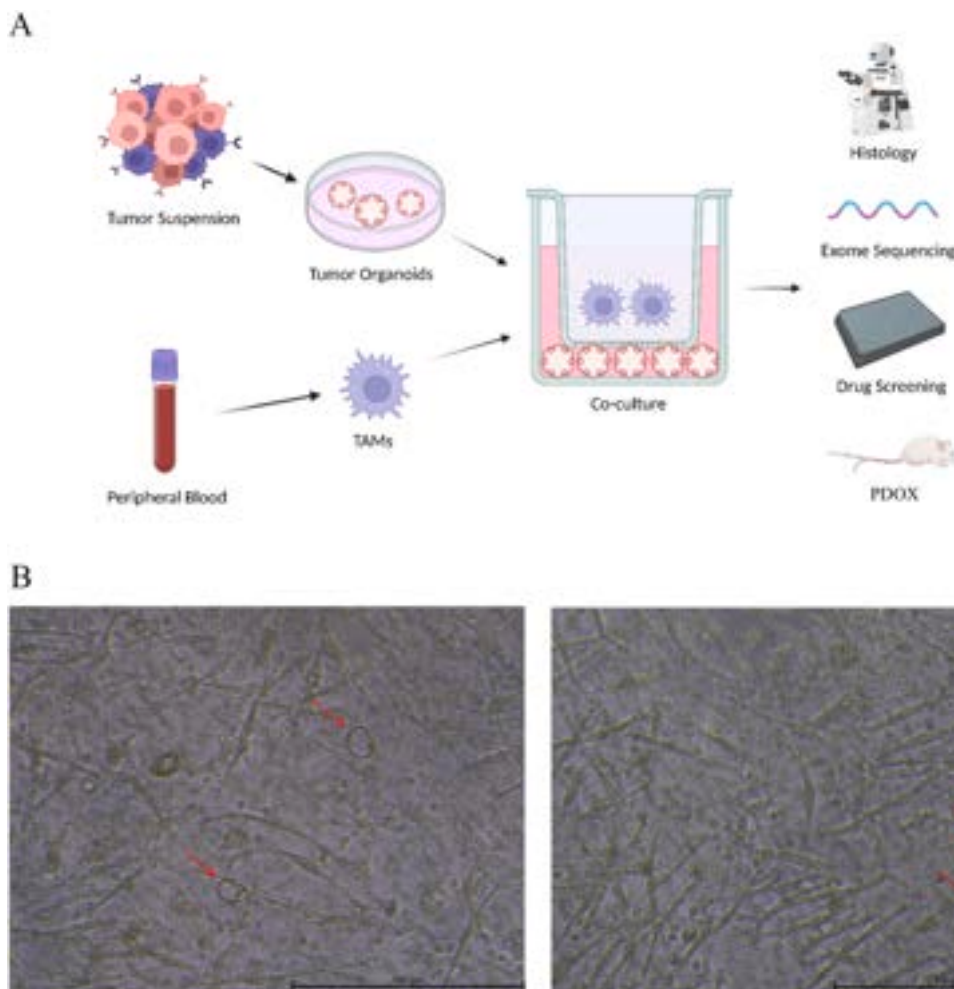


Fig. 1. Construction of extrahepatic cholangiocarcinoma organoids and TAMs co-culture system. (A) Study design used to create co-culture system from eCCA patients. (B) Morphology of eCCA organoids with TAMs in bright field. Organoids had a round structure (red arrow), and TAMs had a spindle structure. (magnification, 100 \times).

Table 1
Description of clinical characteristics of patients involved in the study.

Patient No.	Age	Gender	Tumor Size (cm)	Histological Grade	TNM Stage
Patient 1	64	Male	2	Moderate	T3N0M0
Patient 2	68	Female	8	Poor	T2N0M0
Patient 3	55	Male	1.5	Moderate	T2N1M0
Patient 4	56	Female	10	Moderate	T2N0M0
Patient 5	72	Female	3	Moderate	T2N0M0
Patient 6	78	Female	4.5	Poor	T4N1M0

classical morphological structure of adenocarcinoma. The organoid morphology for P3, P4, and P5 was significantly larger in co-culture than mono-culture, and the nuclei were larger and deeply stained with a higher nucleo-cytoplasm ratio. We next measured the expression of eCCA molecular marker proteins and found that CK7, MUC-1, and EPCAM expression patterns were consistent in the organoids and original tumors. In addition, the expression levels of three organoid markers for P3 were significantly higher in co-culture than mono-culture (Fig. 2C). For patient P5, EPCAM expression was higher in mono-culture than in co-culture, but this

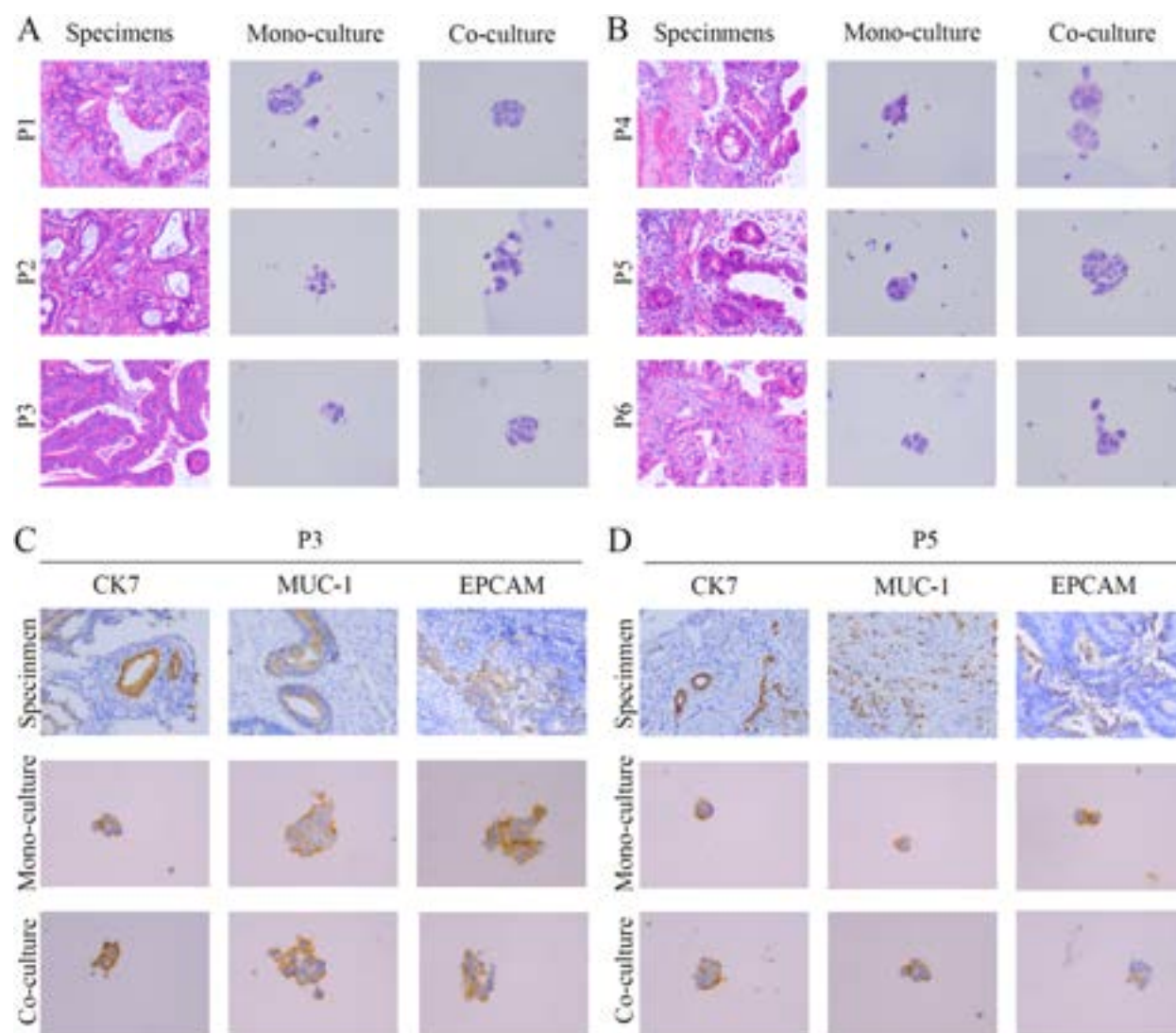


Fig. 2. Histopathological characterization comparing eCCA organoids from mono-culture and co-culture models and corresponding specimens. (A–B) Representative H&E staining of eCCA specimens and organoids (specimen magnification, 200 \times ; organoid magnification, 400 \times). (C–D) Representative immunohistochemistry staining for CK7, MUC-1, and EPCAM in eCCA specimens and organoids (specimen magnification, 200 \times ; organoid magnification, 400 \times).

expression was weak in the original tumor (Fig. 2D & Supplement4). For the other specimens, CK7, MUC-1, and EPCAM expression levels were not significantly different between the two culture models. EPCAM is a cell surface glycoprotein that is overexpressed in a variety of epithelial-derived tumors. A number of previous studies have confirmed that the expression level of EPCAM in tumor cells is

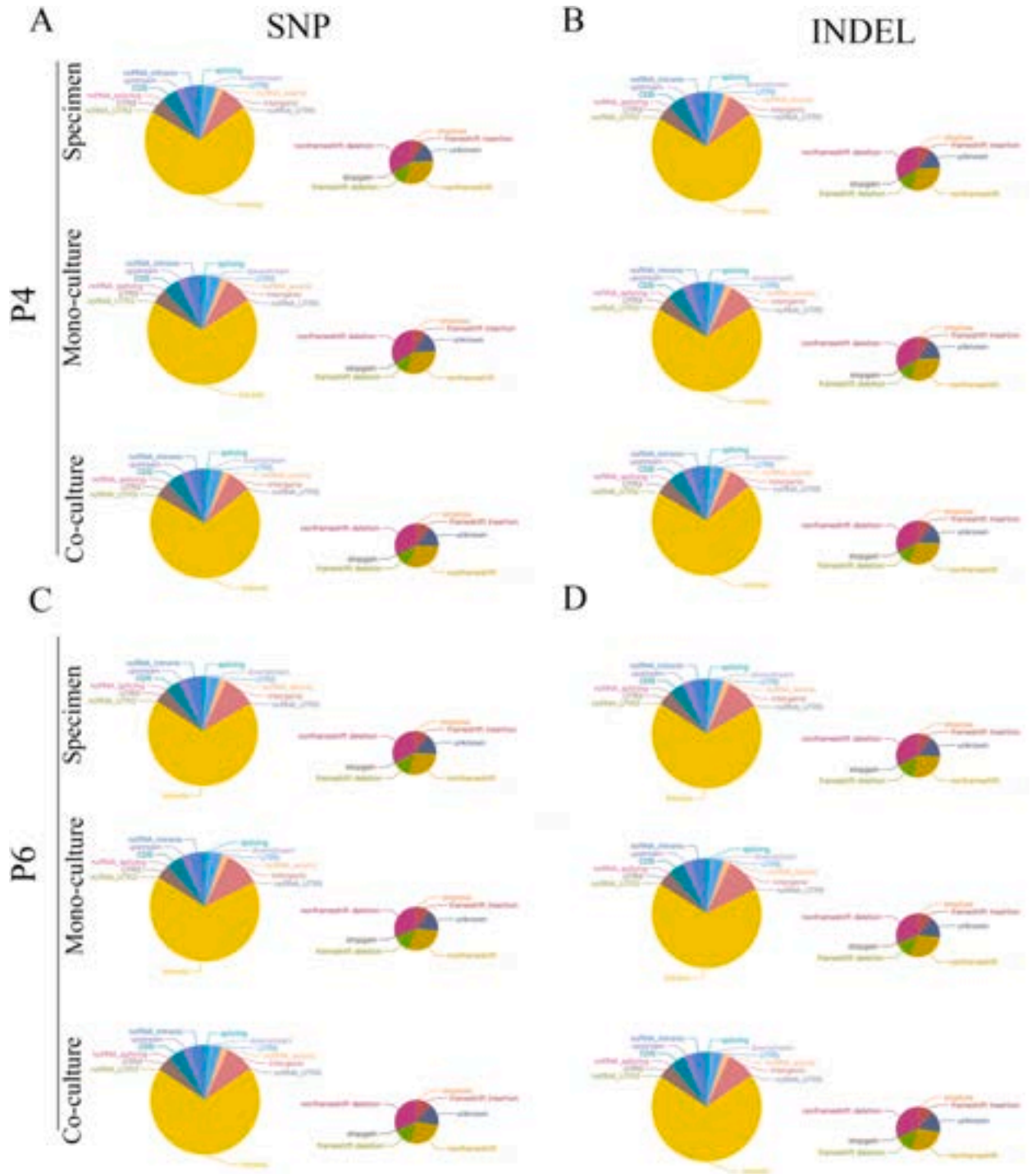


Fig. 3. General genetic alterations in two original specimens and organoids. (A) Number of SNP in different regions of the genome (left) and number of different types of SNP in the coding region (right) from patients 4. (B) Number of INDEL in different regions of the genome (left) and number of different types of INDEL in the coding region (right) from patients 4. (C) Number of SNP in different regions of the genome (left) and number of different types of SNP in the coding region (right) from patients 6. (D) Number of INDEL in different regions of the genome (left) and number of different types of INDEL in the coding region (right) from patients 6.

closely related to tumor invasion, metastasis and prognosis [16]. However, it has not been confirmed that TAMs can directly regulate the expression of EPCAM in tumor cells, but considering that TAMs can secrete a variety of signaling molecules to affect the signaling pathways of tumor cells, we believe that in the future, we can screen the signaling factors secreted by TAMs to explore their role in regulating the expression of EPCAM in the tumor microenvironment of cholangiocarcinoma. Overall, the two organoid culture models retained the histopathologic structures of the tumors, thus preserving homology with the original individual. Notably, the addition of TAMs to the culture system may affect the expression of some representative markers through a yet unknown mechanism.

3.3. Genetic profiles of eCCA organoids

To confirm whether the two culture models recapitulated the genome of the corresponding patient’s tumors, we performed whole-exome sequencing (WES) of DNA from the organoids and original tumors. There were six types of point mutation variations: C > A/G > T, C > G/G > C, C > T/G > C, C > T/G > A, T > A/A > T, and T > C/A > G > C. Initially, we analyzed the mutation characteristics of the 6 groups of eCCA samples. The results showed that C > T/G > A overexpression and T > C/A > G transversions were the most

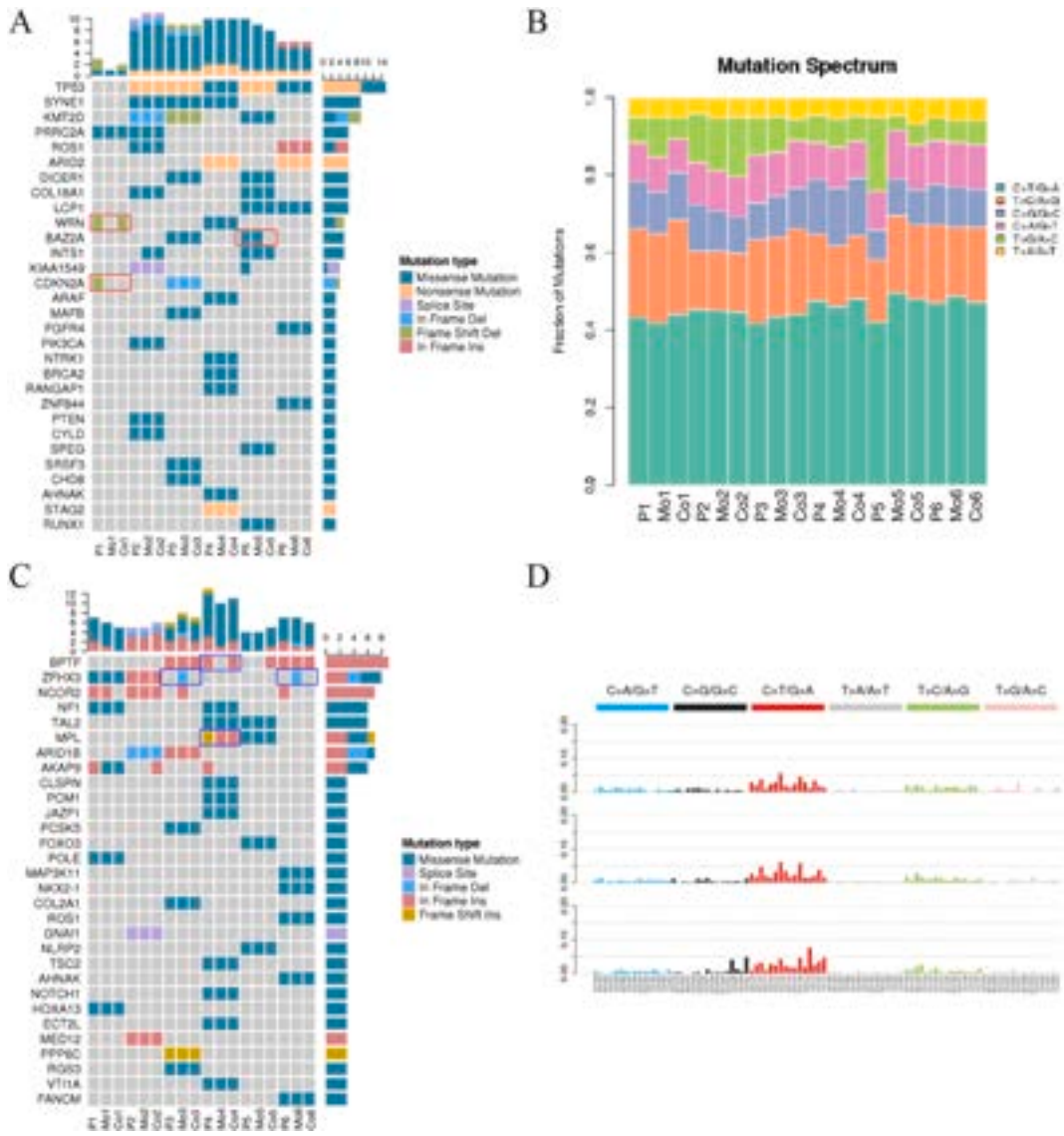


Fig. 4. Detailed genetic profiles of six original specimens and organoids. (A) Representative driver genes of the specimens and organoids are presented. The horizontal coordinate is the sample (P: specimens; Mo: monocultured organoids; Co: co-cultured organoids); the vertical coordinate is the gene; the top is the number of gene mutations in each sample; the right is the number of mutations in each gene in these samples presented. (B) Representative mutation spectrum in the specimens and organoids are presented. (C) Representative cancer predisposition genes in the specimens and organoids are presented. (D) Mutation characteristics of the specimens and organoids are presented.

common (Fig. 4B and D). Then, the mutation spectrums of the organoids of the two models were compared with those of the original tumors. Both culture models retained the genetic spectrum of the original tumors, and in patients P4 and P6, the organoids co-cultured with TAMs had higher reducibility than those mono-cultured. The numbers of SNP and INDEL variations in different regions of the genome and the number of different types of SNP and INDEL variations in coding regions are shown in Fig. 3A–D. Further analysis showed that compared to SNP, INDEL similarity between the organoids and original samples was higher, regardless of genome or coding region and number or characteristics. However, the mono-culture and co-culture models from P1 and P5 patients did not reach the reduction degree of the other 4 cases (Supplement 2). Meanwhile, we statistically analyzed the mutation frequency of tumor cells in the two models, and the results showed that the mutation characteristics of the co-culture group and the original tumor were consistent up to 86.78 %, while the single culture group was 81.84 %. Therefore, the introduction of tumor-associated macrophages into the organoid model in this study was able to improve the reducibility of the model.

Next, we obtained the driver genes of each group to verify their similarity between the organoids and original tumors in different

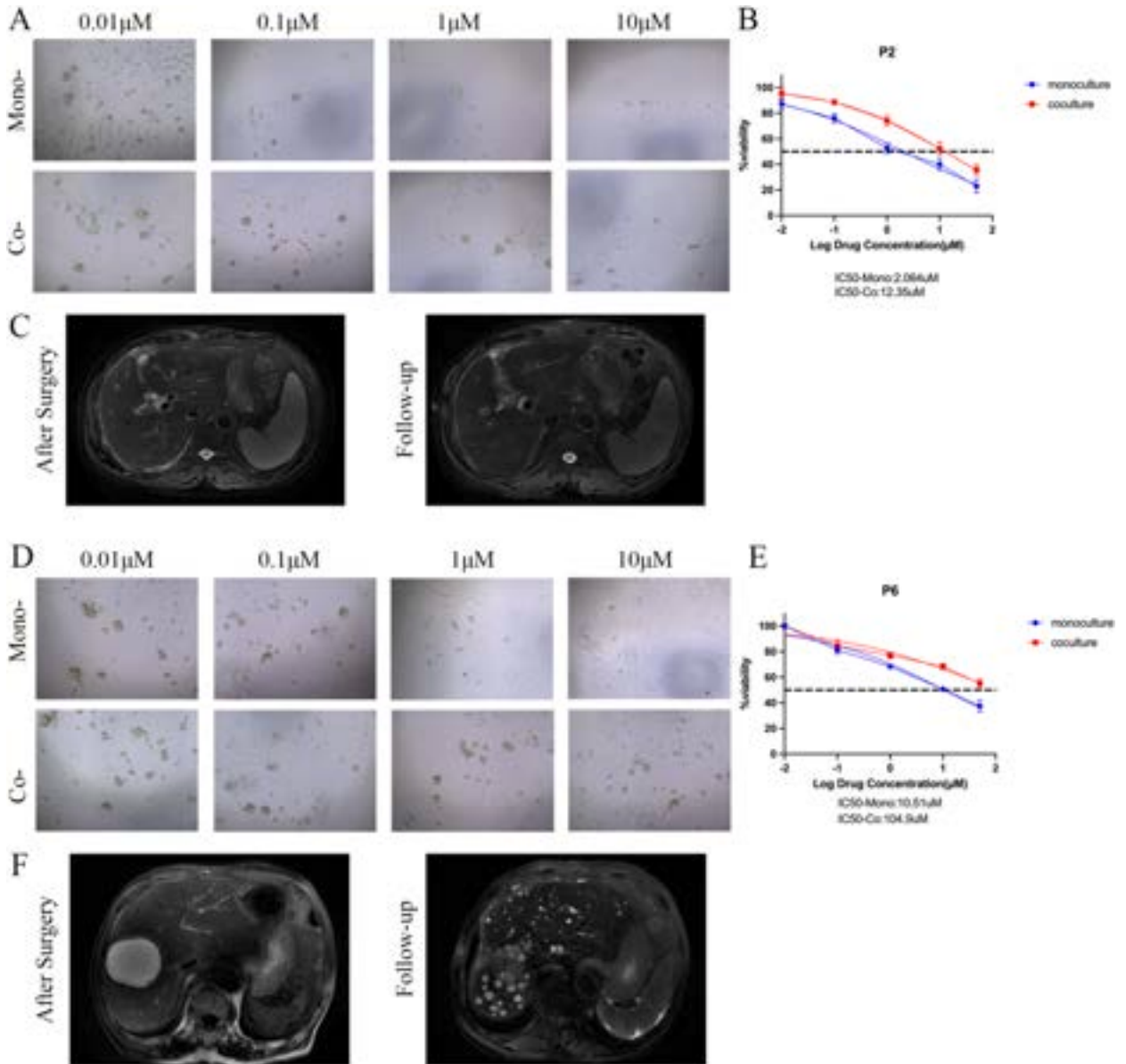


Fig. 5. Organoids response to gemcitabine and cisplatin. (A) Representative images showing patient 2 organoids from the two models response to gemcitabine (magnification, 100×). (B) Dose-response curves of organoids chemosensitivity to gemcitabine. Data are expressed as means ± SD. (C) Representative MR Images of patient 2 during follow-up. (D) Representative images showing patient 6 organoids from the two models response to cisplatin (magnification, 100×). (E) Dose-response curves of organoids chemosensitivity to cisplatin. Data are expressed as means ± SD. (F) Representative MR Images of patient 6 during follow-up.

culture models. We accomplished this by comparing the screened somatic mutations with known driver genes in the database. The results showed that the genetic variations of organoids mono-cultured and co-cultured were mostly consistent with the genetic variations of the original tumors; eCCA was dominated by missense mutations, and 5 patients had TP53 mutations. Among them, the original tumor of patient P1 had a frameshift deletion mutation of WRN, and this mutation was retained in only co-cultured organoids. The organoids of neither model retained the CDKN2A frameshift deletion mutation, which may require medium optimization to improve the reducibility of the model. However, the BAZ2A missense mutation of patient P5 was retained in organoids cultured alone, but not in those co-cultured; this result may be attributed to the addition of TAMs (Fig. 4A). We then screened the mutated genes of each sample for possible cancer predisposition genes. Co-cultured organoids retained the BPTF full code mutation of patient 5, while the MPL mutation type was changed in both mono-culture and co-culture models; the same phenomenon was also found in patient P1. Interestingly, ZHFX3 whole code mutations were present in the mono-culture models of patients P3 and P6 but not in the original

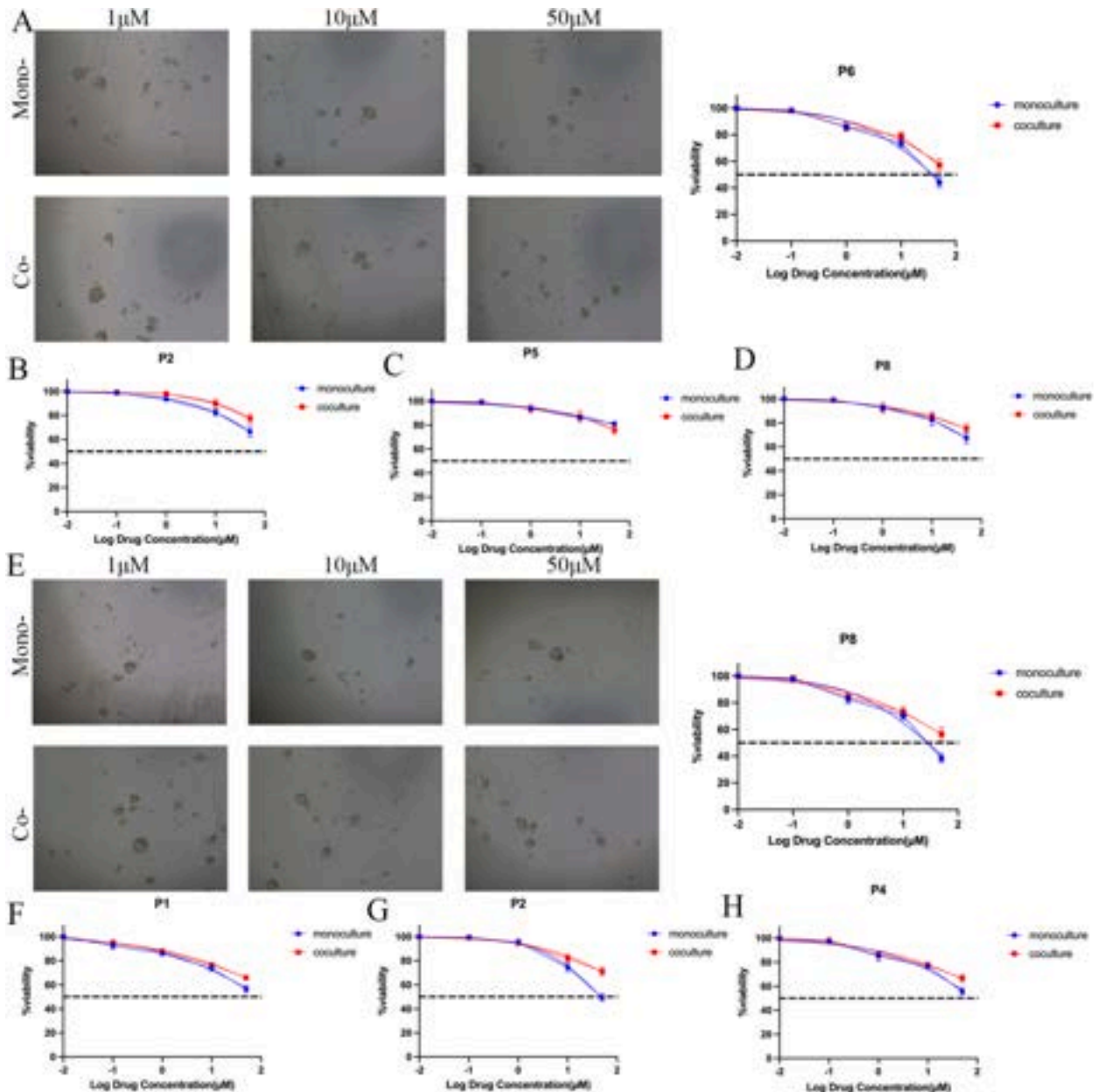


Fig. 6. Organoids response to 5-fluorouracil and paclitaxel. (A) Representative images showing patient 6 organoids from the two models response to 5-fluorouracil(magnification, 100×). (B–D) Dose-response curves of organoids chemosensitivity to 5-fluorouracil. Data are expressed as means ± SD. (E) Representative images showing patient 8 organoids from the two models response to paclitaxel(magnification, 100×). (F–H) Dose-response curves of organoids chemosensitivity to paclitaxel. Data are expressed as means ± SD.

tumors or co-culture models (Fig. 4C). In short, both mono-culture and co-culture models successfully captured intra-patient and inter-patient heterogeneity, but mutations inconsistent with the original tumors appeared for several organoids; this remains a difficult problem to be solved in reconstructing the tumor microenvironment.

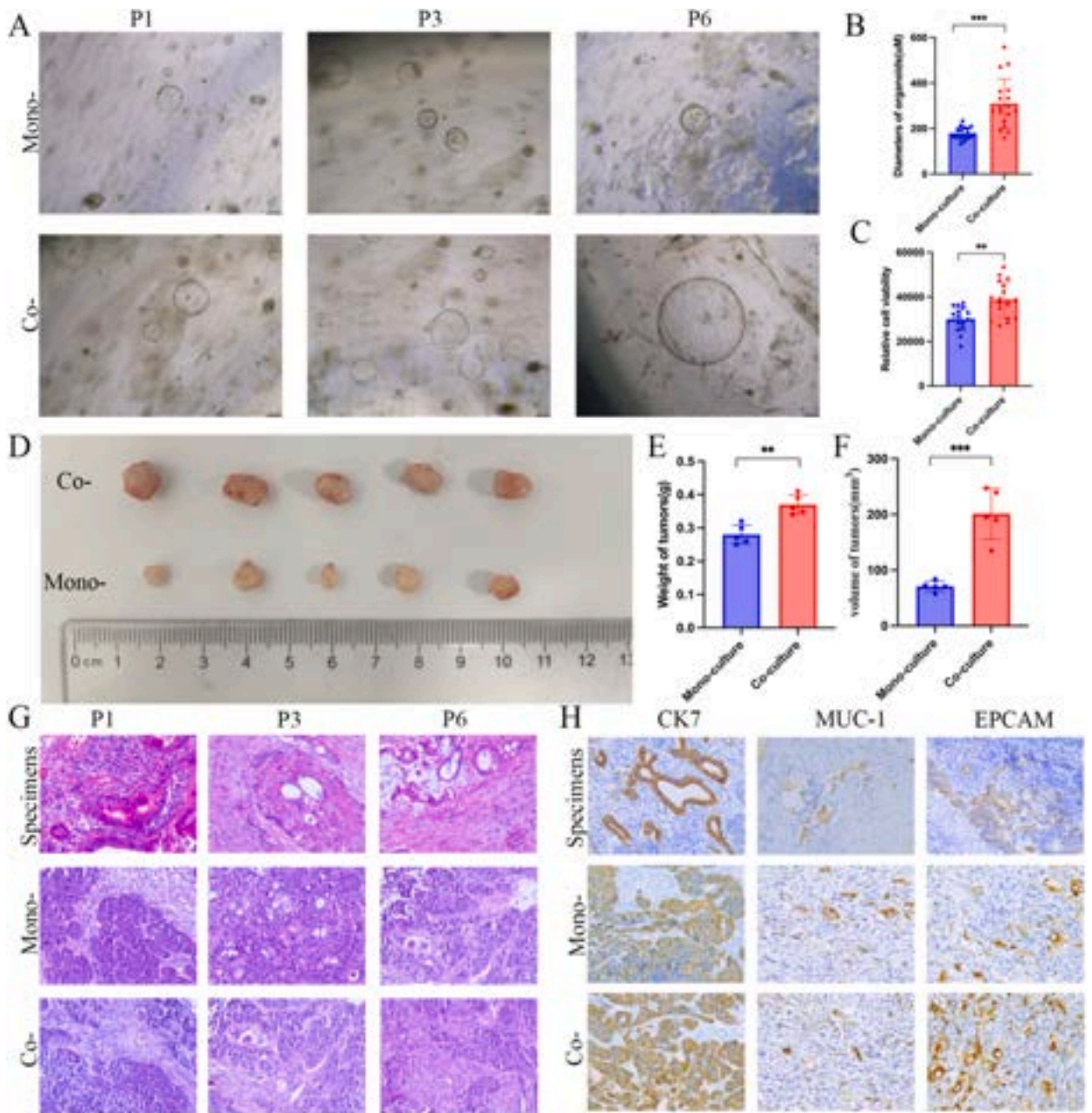


Fig. 7. TAMs promotes the growth of eCCA organoids in vitro and in vivo. (A) Representative images of eCCA organoids in mono-culture and co-culture (magnification, 40 \times). (B) Diameters of eCCA organoids cultured with or without TAMs ($n = 6$, 3 organoids for each well randomly were measured, ** $P < 0.01$, *** $P < 0.001$). Data are expressed as means \pm SD. (C) Cell viability of eCCA organoids cultured with or without TAMs ($n = 6$ experimental settings with 3 biological replicates for each; ** $P < 0.01$, *** $P < 0.001$). Data are expressed as means \pm SD. (D) Representative images of the tumors from mono-transplantation and co-transplantation. (E–F) Weights and volumes of tumors from mono-transplantation and co-transplantation ($n = 5$, ** $P < 0.01$, *** $P < 0.001$). Data are expressed as means \pm SD. (G) Representative H&E staining of tumors from specimens, mono-transplantation, and co-transplantation. (H) Representative immunohistochemistry staining for CK7, MUC-1, and EPCAM in tumors from specimens, mono-transplantation and co-transplantation (magnification, 200 \times).

3.4. TAMs protect eCCA organoids from drug treatment

Next, we measured cell viability to determine the effect of TAMs on eCCA organoids sensitivity to drugs, including gemcitabine, cisplatin, paclitaxel, and 5-fluorouracil (5-FU). Of the 6 eCCA patients, P2 and P6 were sensitive to gemcitabine (Fig. 5A) and cisplatin (Fig. 5D), respectively. However, compared with mono-cultured organoids, organoids co-cultured with TAMs showed decreased sensitivity to gemcitabine and cisplatin (Fig. 5B and E). According to the BILCAP study, patients with recurrence of cholangiocarcinoma within 17.5 months after radical resection were defined as patients with poor clinical response to adjuvant therapy, that is, drug resistant patients [17]. Based on the results of drug susceptibility testing, $IC_{50} \geq 20 \mu M$ was considered as the response of tumor cells to the drug as resistant. The latest follow-up results showed that the P2 patient chose gemcitabine + paclitaxel adjuvant therapy after surgery, and no tumor recurrence was found after surgery (Fig. 5C and D). The two kinds of organ models showed that they were sensitive to gemcitabine. The P6 patient received adjuvant therapy with gemcitabine and cisplatin after surgery, but the patient experienced tumor recurrence 4 months after surgery (Fig. 5F). The IC_{50} of cisplatin in the co-culture model was $109.4 \mu M$, indicating that the co-culture model may have a more accurate prediction of drug response. Gemcitabine and cisplatin drug sensitivity dose curves for the other 3 patients are shown in Supplement 3.

We also explored the dose-response curves of the organoids resistant to the same drug in two models. The responses of P6 to 5-FU and P8 to paclitaxel are shown in Fig. 6A and E, respectively. Although organoids in both models were insensitive to the drugs, cell viability was significantly higher in the co-cultured group at the same dose. The dose-response curves to 5-FU and paclitaxel for the other 3 patients are shown in Fig. 6B–D and Fig. 6F–H, respectively. According to the above results, regardless of whether the organoids are sensitive to drugs or not, the addition of TAMs will make eCCA organoids have higher cell viability and resistance to drugs.

3.5. TAMs promote eCCA organoids growth

In order to explore the influence of TAMs on tumor organoids, the medium selected in the co-culture system was the same as that in the mono-culture system, and the frequency of culture medium replacement and passage were the same. After 14 days of organoids culture, we measured the diameters of 3 random organoids formed in each well for both mono-culture and co-culture models (Fig. 7A). Compared to mono-cultured organoids, organoids co-cultured with TAMs had significantly higher cell viability and significantly larger diameters; the organoids with the largest diameter was co-cultured from patient 6 and reached nearly $600 \mu m$. These results indicated that TAMs promoted eCCA organoids formation (Fig. 7B and C). In order to explore the effect of tumor-associated macrophages on cholangiocarcinoma during the co-culture process, we detected the cytokine concentration in the media of the mono-culture group and the co-culture group. The results showed that the concentrations of IL-10, IL-13, IL-4, FGF, TGF- β , IL-6, VEGF, PDGF and IL-5 in the medium of the co-culture group were significantly higher than those of the single culture group, while IL-12 was higher in the mono-culture group (Supplement 5). Then, we used the PDOX model to explore the effect of TAMs on organoids tumor growth in vivo. Co-transplantation of eCCA organoids with TAMs resulted in more significant tumors than mono-transplantation (Fig. 7D), and the tumors of the co-transplantation group were larger in volume and significantly heavier in weight (Fig. 7E and F). To further verify the histopathological features of the organoids, H&E and immunohistochemical staining were performed (Fig. 7G and H). Immunohistochemical results showed that CK7 and EPCAM expression was significantly higher in the co-transplantation group than the mono-transplantation group. Therefore, these results suggested that TAMs promote organoid growth and influence the expression of some markers of eCCA.

4. Discussion

Tumor organoids are tumor models in which tumor cells grow and form 3D structures on matrix glue or collagen matrix scaffolds. A number of previous studies have confirmed that tumor organoids can retain the tissue structure characteristics and genetic spectrum of source tumors, including colon, ovarian, gastric, and lung cancers, and they can accurately predict drug sensitivity to a certain extent, which has potential value for clinical treatment [16–20]. However, current tumor organoid models are limited by their inability to simulate tumor microenvironments, including the presence of immune cells or fibroblasts, which greatly limits their clinical application. Current studies indicate two methods for preserving or reconstructing the tumor microenvironment using tumor organoid models: first, collagenase use is avoided for tumor digestion and separation to preserve immune cells in the tumor tissue as much as possible; second, immune cells from peripheral blood can be added for co-culture with organoids to restore the interactions between immune cells and tumor cells and reconstruct the tumor immune microenvironment to a certain extent [13,21]. In this study, we successfully established a tumor organoid model of co-culture with eCCA and TAMs derived from peripheral blood. We demonstrated that this tumor model can reproduce inter-patient heterogeneity to a certain extent.

Cancer stem cells are self-renewing cell populations involved in tumor genesis, metastasis, and drug resistance [18]. Previous studies have found co-localization of TAMs and cancer stem cell-related markers (CD44 or EPCAM) via immunostaining in CCA, suggesting a potential association between the two [19]. In our study, we also found that EPCAM expression was higher in the co-culture model. Although the underlying mechanism has not yet been studied, this provides new evidence for the interaction between TAMs and tumor stem cells in the tumor microenvironment. Recently, Hee et al. classified ICC patients into Small-Duct (SD) and Large-Duct (LD) subtypes based on the expression of S100P, N-cadherin, and CD56 [20]. Such phenotypic heterogeneity may also exist in the organoid model we established, and whether TAMs play a role in these histological features requires further future exploration.

Due to the lack of tumor microenvironment, some tumor organoids cannot fully reproduce the genetic characteristics of the original

tumor [21]. We comprehensively analyzed the genetic profiles of the CCA cells in both models by exon sequencing and compared them with the original tumors. The results showed that both models retained the basic genetic profiles of the original tumors. However, in some samples, the co-culture of CCA organoids with TAMs yielded greater consistency than the mono-culture model, and the specific mutation characteristics of the samples were preserved. We believe that the co-culture model captures intra- and inter-patient heterogeneity to some extent, which can not only improve model reducibility but also yield a research tool for examining the interactions between TAMs and CCA cells. Future studies reconstructing the tumor organoid immune microenvironment still need to introduce other cells into the tumor microenvironment and optimize the organoid medium components to better improve the precision of drug sensitivity screening. A recent study found that tumor-associated fibroblasts in the tumor microenvironment promoted the growth of liver tumor organoids, but the reducibility of the co-culture model was not verified [22].

Genomic heterogeneity exists in the tumors of CCA patients, which results in different chemotherapy responses. In addition, genetic mutations within tumors often lead to the emergence of drug resistance. In our study, four common chemotherapy drugs were used for screening. The results showed that no matter whether the organoids in the mono-culture model were sensitive to drugs or not, the corresponding organoids co-cultured with TAMs were less sensitive, indicating that TAMs play a role in chemotherapy drug resistance in the eCCA organoid model. Two organoids sensitive to gemcitabine and cisplatin were selected to construct the PDOX model, and the drug sensitivity results confirmed the role of TAMs in treatment resistance. Previous studies have found that tumor-associated macrophages are involved in bile duct cancer progression and gemcitabine resistance [23]. Combined with our previous studies, we believe that the eCCA organoid model can predict chemotherapy responses to a certain extent, but tumor heterogeneity and drug resistance development over time require longer follow-up verification [14]. At the same time, when constructing the co-culture model, we found that TAMs could promote tumor organoid growth and shorten the organoid construction cycle. The co-culture model can be used to summarize the effect of TAMs in promoting organoid growth and therapeutic resistance. However, the molecular mechanisms of these effects remain to be determined.

Here, we successfully constructed an organoid model where TAMs and eCCA from the same patient are co-cultured, providing a valuable research tool for the further optimization of tumor organoid models and examination of the interactions between TAMs and eCCA. Notably, the lack of other immune cells and stromal cells weakens the impact of this study to some extent, but the drug sensitivity results of the current model could begin to guide clinical drug use. In conclusion, more prospective multicenter data are needed to validate our findings. Furthermore, introduction of additional tumor microenvironment components and optimization of the culture medium are needed to advance the further development of tumor organoid models, which could have a potential role in predicting drug responses in eCCA patients.

5. Conclusions

Currently, tumor organoids are widely used in drug screening, but the accuracy of drug sensitivity is limited by the lack of tumor microenvironment in models. In this paper, monocytes from peripheral blood of patients were induced into tumor-associated macrophages and co-cultured with extracellular cholangiocarcinoma organoids. It was confirmed that this co-culture model can better capture intra- and inter-tumor heterogeneity, and it was found that tumor macrophages promoted tumor proliferation and chemotherapy resistance in the tumor microenvironment. Overall, our results suggest that this co-culture model is a promising preclinical tumor model.

Ethics approval and consent to participate

The animal experiments in this study was approved by the ethics committee of the Second Affiliated Hospital, Zhejiang University, School of Medicine (No. 2024-021).

And the human experiments in this study was approved by the ethics committee of the Second Affiliated Hospital, Zhejiang University, School of Medicine (No. 2019–2408).

Funding

This research was supported by the Major science and technology program of Fujian Province under Grant [2021YZ036017]; and the Natural Science Foundation of Zhejiang Province under Grant [LY19H160053].

Availability of data and materials

The raw sequence data reported in this paper have been deposited in the Genome Sequence Archive in the National Genomics Data Center, China National Center for Bioinformation/Beijing Institute of Genomics, Chinese Academy of Sciences (HRA005181), which is publicly accessible at <https://ngdc.cncb.ac.cn/gsa>.

CRediT authorship contribution statement

Yinghao Guo: Writing – original draft, Methodology, Investigation, Formal analysis, Data curation, Conceptualization. **Qi Li:** Writing – original draft, Methodology, Investigation, Conceptualization. **Qinghuang Ye:** Writing – review & editing, Resources, Investigation. **Yun Jin:** Resources. **Yuanquan Yu:** Resources. **Xiaoxiao Zhang:** Resources, Methodology. **Longfu Xi:** Resources.

Yihang Wang: Resources. **Di Wu:** Resources. **Yanzhi Pan:** Resources. **Shumei Wei:** Funding acquisition, Data curation. **Qingyong Li:** Visualization, Supervision. **Huiquan Wang:** Visualization, Supervision. **Jiangtao Li:** Writing – review & editing, Visualization, Supervision, Project administration, Funding acquisition.

Declaration of competing interest

The authors declare that they have no known competing financial interests or personal relationships that could have appeared to influence the work reported in this paper.

Acknowledgements

We thank all patients enrolled in this study.

Abbreviations

PDOs	patient-derived organoids
TAMs	tumor-associated macrophages
5-FU	5-fluorouracil
eCCA	extrahepatic cholangiocarcinoma
M1	classically activated macrophages
M2	alternately activated macrophages
PDX	patient-derived tumor xenograft
PBMCs	peripheral blood mononuclear cells
PDOX	patient-derived organoid xenograft

Appendix A. Supplementary data

Supplementary data to this article can be found online at <https://doi.org/10.1016/j.heliyon.2024.e36377>.

References

- [1] P. Bertuccio, M. Malvezzi, G. Carioli, D. Hashim, P. Boffetta, H.B. El-Serag, C. La Vecchia, E. Negri, Global trends in mortality from intrahepatic and extrahepatic cholangiocarcinoma, *J. Hepatol.* 71 (1) (2019) 104–114.
- [2] L. Fabris, M.J. Perugorria, J. Mertens, N.K. Björkström, T. Cramer, A. Lleo, A. Solinas, H. Sängler, V. Lukacs-Kornek, A. Moncsek, A. Siebenhüner, M. Strazzabosco, The tumour microenvironment and immune milieu of cholangiocarcinoma, *Liver Int.* 39 (Suppl 1) (2019) 63–78.
- [3] D. Sun, T. Luo, P. Dong, N. Zhang, J. Chen, S. Zhang, L. Liu, L. Dong, S. Zhang, CD86+/CD206+ tumor-associated macrophages predict prognosis of patients with intrahepatic cholangiocarcinoma, *PeerJ* 8 (2020) e8458.
- [4] F. Tacke, Targeting hepatic macrophages to treat liver diseases, *J. Hepatol.* 66 (6) (2017) 1300–1312.
- [5] L. Kong, Y. Zhou, H. Bu, T. Lv, Y. Shi, J. Yang, Deletion of interleukin-6 in monocytes/macrophages suppresses the initiation of hepatocellular carcinoma in mice, *J. Exp. Clin. Cancer Res.* 35 (1) (2016) 131.
- [6] M. Schulz, A. Salamero-Boix, K. Niesel, T. Alekseeva, L. Sevenich, Microenvironmental regulation of tumor progression and therapeutic response in brain metastasis, *Front. Immunol.* 10 (2019) 1713.
- [7] H. Prenen, M. Mazzone, Tumor-associated macrophages: a short compendium, *Cell. Mol. Life Sci.* 76 (8) (2019) 1447–1458.
- [8] M. van de Wetering, H.E. Francies, J.M. Francis, G. Bounova, F. Iorio, A. Pronk, W. van Houdt, J. van Gorp, A. Taylor-Weiner, L. Kester, A. McLaren-Douglas, J. Blokker, S. Jaksani, S. Bartfeld, R. Volckman, P. van Sluis, V.S.W. Li, S. Seepo, C. Sekhar Pedamallu, K. Cibulskis, S.L. Carter, A. McKenna, M.S. Lawrence, L. Lichtenstein, C. Stewart, J. Koster, R. Versteeg, A. van Oudenaarden, J. Saez-Rodriguez, R.G.J. Vries, G. Getz, L. Wessels, M.R. Stratton, U. McDermott, M. Meyerson, M.J. Garnett, H. Clevers, Prospective derivation of a living organoid biobank of colorectal cancer patients, *Cell* 161 (4) (2015) 933–945.
- [9] N. Sachs, J. de Lig, O. Kopper, E. Gogola, G. Bounova, F. Weeber, A.V. Balgobind, K. Wind, A. Gracanin, H. Begthel, J. Korving, R. van Boxtel, A.A. Duarte, D. Lelieveld, A. van Hoeck, R.F. Ernst, F. Blokzijl, I.J. Nijman, M. Hoogstraat, M. van de Ven, D.A. Egan, V. Zinzalla, J. Moll, S.F. Boj, E.E. Voest, L. Wessels, P. J. van Diest, S. Rottenberg, R.G.J. Vries, E. Cuppen, H. Clevers, A living biobank of breast cancer organoids captures disease heterogeneity, *Cell* 172 (1–2) (2018) 373–386.e10.
- [10] D.P. Kodack, A.F. Farago, A. Dastur, M.A. Held, L. Dardaei, L. Friboulet, F. von Flotow, L.J. Damon, D. Lee, M. Parks, R. Dicecca, M. Greenberg, K.E. Kattermann, A.K. Riley, F.J. Fintelmann, C. Rizzo, Z. Piotrowska, A.T. Shaw, J.F. Gainor, L.V. Sequist, M.J. Niederst, J.A. Engelman, C.H. Benes, Primary patient-derived cancer cells and their potential for personalized cancer patient care, *Cell Rep.* 21 (11) (2017) 3298–3309.
- [11] E. Fiorini, L. Veghini, V. Corbo, Modeling cell communication in cancer with organoids: making the complex simple, *Front. Cell Dev. Biol.* 8 (2020) 166.
- [12] D. Öhlund, A. Handy-Santana, G. Biffi, E. Elyada, A.S. Almeida, M. Ponz-Sarvisé, V. Corbo, T.E. Oni, S.A. Hearn, E.J. Lee, I.I.C. Chio, C.-I. Hwang, H. Tiriác, L. A. Baker, D.D. Engle, C. Feig, A. Kultti, M. Egeblad, D.T. Fearon, J.M. Crawford, H. Clevers, Y. Park, D.A. Tuveson, Distinct populations of inflammatory fibroblasts and myofibroblasts in pancreatic cancer, *J. Exp. Med.* 214 (3) (2017) 579–596.
- [13] K.K. Dijkstra, C.M. Cattaneo, F. Weeber, M. Chalabi, J. van de Haar, L.F. Fanchi, M. Slagter, D.L. van der Velden, S. Kaing, S. Kelderman, N. van Rooij, M.E. van Leerdaam, A. Depla, E.F. Smit, K.J. Hartemink, R. de Groot, M.C. Wolkers, N. Sachs, P. Snaebjornsson, K. Monkhorst, J. Haanen, H. Clevers, T.N. Schumacher, E. E. Voest, Generation of tumor-reactive T cells by Co-culture of peripheral blood lymphocytes and tumor organoids, *Cell* 174 (6) (2018) 1586–1598.e12.
- [14] Z. Wang, Y. Guo, Y. Jin, X. Zhang, H. Geng, G. Xie, D. Ye, Y. Yu, D. Liu, D. Zhou, B. Li, Y. Luo, S. Peng, J. Li, Establishment and drug screening of patient-derived extrahepatic biliary tract carcinoma organoids, *Cancer Cell Int.* 21 (1) (2021) 519.
- [15] Z. Wang, Y. Jin, Y. Guo, Z. Tan, X. Zhang, D. Ye, Y. Yu, S. Peng, L. Zheng, J. Li, Conversion therapy of intrahepatic cholangiocarcinoma is associated with improved prognosis and verified by a case of patient-derived organoid, *Cancers* 13 (5) (2021) 1179.
- [16] M.A. Mohtar, S.E. Syafruddin, S.N. Nasir, T.Y. Low, Revisiting the roles of pro-metastatic EpCAM in cancer, *Biomolecules* 10 (2) (2020) 255.

- [17] J.N. Primrose, R.P. Fox, D.H. Palmer, H.Z. Malik, R. Prasad, D. Mirza, A. Anthony, P. Corrie, S. Falk, M. Finch-Jones, H. Wasan, P. Ross, L. Wall, J. Wadsley, J.T. R. Evans, D. Stocken, R. Praseedom, Y.T. Ma, B. Davidson, J.P. Neoptolemos, T. Iveson, J. Raftery, S. Zhu, D. Cunningham, O.J. Garden, C. Stubbs, J.W. Valle, J. Bridgewater, BILCAP study group, Capecitabine compared with observation in resected biliary tract cancer (BILCAP): a randomised, controlled, multicentre, phase 3 study, *Lancet Oncol.* 20 (5) (2019) 663–673.
- [18] H.-J. Wu, P.-Y. Chu, Role of cancer stem cells in cholangiocarcinoma and therapeutic implications, *Int. J. Mol. Sci.* 20 (17) (2019) 4154.
- [19] C. Raggi, M. Correnti, A. Sica, J.B. Andersen, V. Cardinale, D. Alvaro, G. Chiorino, E. Forti, S. Glaser, G. Alpini, A. Destro, F. Sozio, L. Di Tommaso, M. Roncalli, J.M. Banales, C. Coulouarn, L. Bujanda, G. Torzilli, P. Invernizzi, Cholangiocarcinoma stem-like subset shapes tumor-initiating niche by educating associated macrophages, *J. Hepatol.* 66 (1) (2017) 102–115.
- [20] H.S. Lee, D.H. Han, K. Cho, S.B. Park, C. Kim, G. Leem, D.E. Jung, S.S. Kwon, C.H. Kim, J.H. Jo, H.W. Lee, S.Y. Song, J.Y. Park, Integrative analysis of multiple genomic data from intrahepatic cholangiocarcinoma organoids enables tumor subtyping, *Nat. Commun.* 14 (1) (2023) 237.
- [21] H. Nakamura, M. Sugano, T. Miyashita, H. Hashimoto, A. Ochiai, K. Suzuki, M. Tsuboi, G. Ishii, Organoid culture containing cancer cells and stromal cells reveals that podoplanin-positive cancer-associated fibroblasts enhance proliferation of lung cancer cells, *Lung Cancer* 134 (2019) 100–107.
- [22] J. Liu, P. Li, L. Wang, M. Li, Z. Ge, L. Noordam, R. Lieshout, M.M.A. Versteegen, B. Ma, J. Su, Q. Yang, R. Zhang, G. Zhou, L.C. Carrascosa, D. Sprengers, J.N. M. Ijzermans, R. Smits, J. Kwakkeboom, L.J.W. van der Laan, M.P. Peppelenbosch, Q. Pan, W. Cao, Cancer-associated fibroblasts provide a stromal niche for liver cancer organoids that confers trophic effects and therapy resistance, *Cell Mol Gastroenterol Hepatol* 11 (2) (2021) 407–431.
- [23] T. Yang, Z. Deng, L. Xu, X. Li, T. Yang, Y. Qian, Y. Lu, L. Tian, W. Yao, J. Wang, Macrophages-aPKC-CCL5 feedback loop modulates the progression and chemoresistance in cholangiocarcinoma, *J. Exp. Clin. Cancer Res.* 41 (1) (2022) 23.